ACS APPLIED POLYMER MATERIALS

pubs.acs.org/acsapm

Article

A Green High Barrier Solution for Paperboard Packaging based on Potato Fruit Juice, Poly(lactic acid), and Poly(butylene adipate terephthalate)

Simi Poulose,* Juuso Toriseva, Johanna Lahti, Ilari Jönkkäri, Mikael S. Hedenqvist,* and Jurkka Kuusipalo

Cite This: *ACS Appl. Polym. Mater.* 2022, 4, 4179−4188

Read Online

ACCESS | Metrics & More | Article Recommendations | Supporting Information

ABSTRACT: The potential of using potato fruit juice (PFJ), a byproduct from the potato starch industry, was investigated as a barrier paper-coating material. The paperboard was initially hand-coated with PFJ (with and without glycerol as plasticizer) and then extrusion-coated with poly(lactic acid) (PLA) or a blend of PLA and poly(butylene adipate terephthalate) (PBAT). The multilayer coated paperboard was homogeneous in appearance with a glossy finish. The coated paperboard showed, at the most, a ca. 95% reduction in specific water vapor transmission rate compared to the uncoated paperboard. In the presence of the PFJ layer, the extrusion-coated paperboard experienced, at the most, a 98% reduction in oxygen permeability. The grease resistance of the paperboard was also improved significantly with this multilayer coating. PLA- and PFJ-coated samples showed better barrier properties, whereas PFJ with PLA/PBAT layers exhibited better adhesion and heat-sealing properties. The peel strength of the coated samples was moderately good for paper converting applications. The developed coated paperboard also exhibited good creasing properties which is yet again an advantage for packaging applications. The presented barrier properties make the developed multilayer coatings on paperboards a sustainable competitive alternative to several of today's coatings.

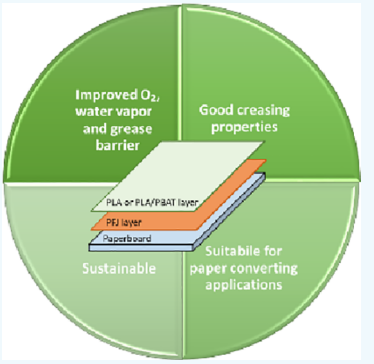

KEYWORDS: *paper coating, barrier coating, bio-based coating, potato fruit juice, poly(lactic acid), poly(butylene adipate terephthalate), barrier properties, peel strength, heat sealing*

1. INTRODUCTION

Owing to its good mechanical properties along with its biodegradable and recyclable nature, paper is widely used as a packaging material. However, for efficient use of paper, especially in food packaging applications, its hydrophilicity and porosity have to be addressed properly. In addition, a good oxygen and grease barrier is often required. This necessitates barrier coating materials for improving barrier properties against oxygen, water vapor, and grease. Synthetic polymers, such as polyethylene, poly(ethylene-*co*-vinyl alcohol) (EVOH), polyvinylidene chloride (PVDC), and waxes are widely used for barrier coating purposes.[1−3]

However, future depleting availability of fossil resources and their effects on the carbon footprint are driving industries to find ecofriendly renewable resources that in turn increase the sustainability. Renewable biopolymers and materials such as proteins,[4−7] polysaccharides,[8] lipids,[9] and polyesters, such as poly(lactic acid) (PLA)[10] and poly(hydroxy butyrate) (PHB) or their combinations,[11−16] are studied to substitute synthetic polymers and as coatings on paper.

An even more sustainable solution is obtained if these bio-based alternatives are produced from industrial byproducts that are otherwise wasted. From this perspective, potato fruit juice (PFJ) was selected as a coating material because it is obtained as a byproduct from the potato starch industry. In the potato starch production, potatoes are first washed and grinded. After passing the rasped potatoes through rotating sieves, the remaining starch slurry is passed through continuous centrifugal separators. The purified slurry is used for potato starch production and the byproduct collected at this step is PFJ. It is available in bulk quantities, from 0.7 to 7 m^3/ton tuber, the specific quantity depending on how it is produced. Its abundant availability and low cost are undoubtedly an advantage. PFJ, with a protein content of 25−30% of the dry matter, is a complex dilute aqueous mixture of many different components, such as protein, peptides, amino acids and amides, sugars, potassium, small amounts of other N-containing compounds, organic acids, lipids, and phosphorus.[17]

Received: January 25, 2022
Accepted: May 4, 2022
Published: May 19, 2022

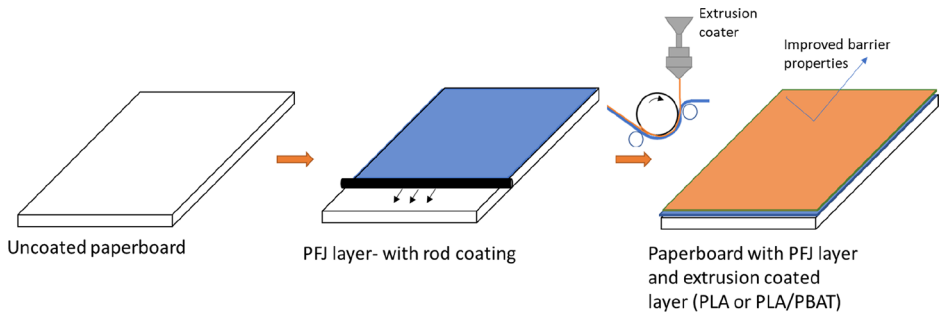

Figure 1. Illustration of the development of the coated paperboard.

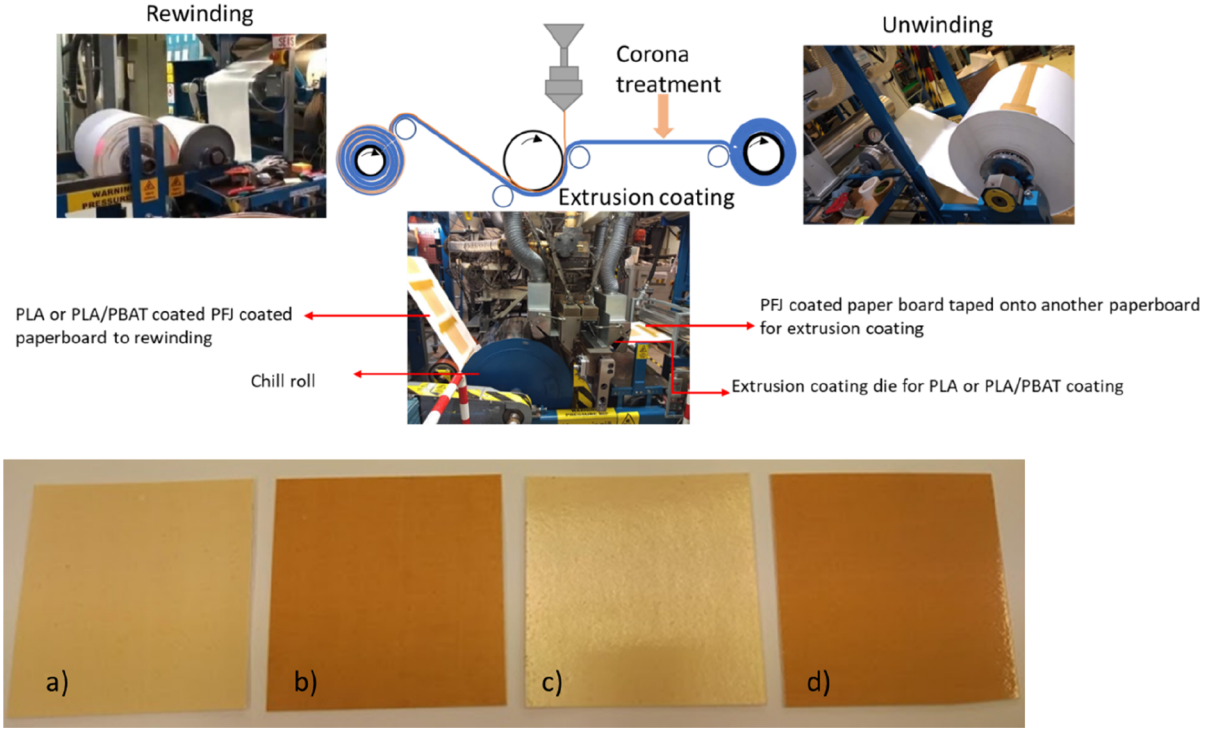

Figure 2. Pilot plant extrusion coater (above) and paperboard with multilayer coating of (a) P0-thin-30PLA, (b) P0-thick-30PLA, (c) P0-thin-30PLA/PBAT, and (d) P0-thick-30PLA/PBAT (below).

In our previous article, PFJ films with and without plasticizer (glycerol) were developed and it was observed that they had remarkably low oxygen permeability (OP) and good grease barrier properties. The good grease barrier was due to the high polarity of PFJ. The polar components and hydrogen bonding species of PFJ also contribute to the high gas/oxygen barrier properties. At the same time, due to the hydrophilicity, the water vapor barrier was, as expected, low.[18] In this study, the use of PFJ as a barrier coating layer on paperboard was evaluated in order to assess its potential as a gas barrier layer in future biobased packaging. In order to protect PFJ from moisture, a multilayer structure was developed where the PFJ layer was covered with a polymer of lower hydrophilicity. The paperboard, solution-coated with PFJ, was extrusion-coated with either PLA or a blend of PLA and poly(butylene adipate terephthalate) (PBAT) (Figure 1). In the PLA/PBAT blend, PBAT is used to improve the toughness of PLA.[19] The morphology of the produced layered materials and their water, oxygen, and grease-barrier properties were evaluated. Physical and packaging-related properties, including layer adhesion, creasing properties, and sealing properties, were also determined, as well as the thermal/calorimetric properties of the two types of extruded materials.

2. EXPERIMENTAL SECTION

2.1. Materials. A pigment-coated paperboard (Ensocoat, Stora Enso) with a grammage of 275 g/m^2 was used as the substrate for the study. This pigment-coated paperboard was selected because of its smoother surface and lower surface porosity compared to the uncoated paperboard. This provided better retention of the PFJ coating on the surface of the board. PFJ was obtained from Finnamyl, with 23 wt % dry solid content (31 wt % of the dry content was protein). Glycerol (≥99.5%) was purchased from Sigma-Aldrich Chemie. For extrusion coating, a PLA (density: 1240 kg/m^3) and a blend of PLA and PBAT (density: 1240−1250 kg/m^3, containing 60% PLA and 40% PBAT) were used. It was observed that the pure PLA and the PLA in the blend were not the same grades.

2.2. Rod Coating. PFJ was coated on the paperboard using a K Hand coater, Print-Coat Instruments Ltd. Prior to the coating, the PFJ was mixed with glycerol to a content of 0, 10, 20, and 30 wt % of its protein content (P0, P10, P20, and P30) as in the previous paper.[18] Coatings were obtained by using a wire bound bar, exerting constant pressure between the bar and paperboard. The PFJ coating was made in two thicknesses, referred to as thin coating and thick coating. The thin

https://doi.org/10.1021/acsapm.2c00153
ACS Appl. Polym. Mater. 2022, 4, 4179−4188

Table 1. Colorimeter Values of the PFJ Coated and Uncoated Paperboards

paperboard	L^*	a^*	b^*	ΔE^*
paperboard-uncoated-reference	95.2 ± 0.0	1.8 ± 0	−6.7 ± 0	0
P0-thin-30PLA	84.8 ± 0.1	2.3 ± 0.1	19.8 ± 0.3	28.5 ± 0.2
P0-thick-30PLA	69.5 ± 0.9	11.4 ± 0.3	36.7 ± 1.1	51.5 ± 0.9
P0-thin-30 PLA/PBAT	84.4 ± 0.2	2.8 ± 0.1	18.6 ± 0.5	27.6 ± 0.3
P0-thick-30 PLA/PBAT	69.9 ± 0.5	11.1 ± 0.2	33.1 ± 2.1	48.2 ± 1.6

coating was obtained by one coating of PFJ on the paperboard, resulting in a thickness on the order of 5 μm. The thick coating was obtained by three coatings on the paperboard. The resulting PFJ layer thickness was on the order of 15 μm. The paperboard was dried in an oven (Memmert UF 160 plus) at 120 °C for 1 min after each layer of coating. The bar used for coating had a 0.31 mm diameter wire wound around it.

2.3. Extrusion Coating. The PFJ-coated paperboards were taped to a paper roll and this was then finally coated with PLA or PLA/PBAT using a pilot plant extrusion coater (Figure 2). Extrusion-coating was done with two different surface weights/grammages (20 g/m^2 and 30 g/m^2) in order to determine the effects of the coating size on the barrier properties. The paperboard was corona-treated (3.4 kW) to improve the adhesion of the polymer to the surface of the PFJ-coated paperboard. Some paperboard samples (taken from the thick PFJ coating and 30 g/m^2 PLA or PLA/PBAT) were coated without corona treatment to study the effect of corona on the adhesion to the paperboard. The nomenclature of the different samples is given in Table S1 and the grammage of these are given in Table S2. For example, "P0-thick" refers to a sample with a thick layer of PFJ (without glycerol) on the paperboard and "P30-thin-30PLA" refers to a sample with a thin PFJ coating (with glycerol 30 wt % protein content of PFJ), having also an extrusion-coated 30 g/m^2 PLA layer on top. All samples were conditioned at 50% RH and 23 °C for at least 3 days prior to all tests.

2.4. Colorimeter. The color measurement, using the CIELAB color space, was carried out with the spectrophotometer CM-3630 Konica Minolta (Japan). The three parameters: L^* (lightness), a^* (negative values indicate green and positive values indicate red), and b^* (negative values indicate blue and positive values indicate yellow) were determined. Five measurements were collected in order to obtain a mean value. The changes in color compared to uncoated paperboard as reference was calculated as total color difference ΔE^* using eq 1.[20]

$$\Delta E^* = \sqrt{(L^* - L^*_{\mathrm{ref}})^2 + (a^* - a^*_{\mathrm{ref}})^2 + (b^* - b^*_{\mathrm{ref}})^2} \quad (1)$$

2.5. Differential Scanning Calorimetry. Differential scanning calorimetry (DSC, NETZSCH DSC 214 Polyma) was used to determine the glass transition temperature and crystallinity of the extruded PLA or PLA/PBAT layers. The extruded layer was peeled off carefully from the paperboard, on samples not treated with corona, and then analysed. Samples weighing 5−10 mg were placed in sealed aluminum pans with pierced lids, along with a reference empty aluminum pan with pierced lid, were heated from −20 to 200 °C at a heating rate of 20 °C min^{-1} in nitrogen (purge gas rate; 40 mL/min).

2.6. Fourier Transform Infrared Spectroscopy. Fourier transform infrared spectroscopy (FTIR)-ATR Spectrum One (PerkinElmer) was used to collect the spectra between 600 and 4000 cm^{-1}. The number of scans used was 64 and the resolution was 4 cm^{-1}.

2.7. Optical Microscopy and Creasing. Cross-sectional images were taken with a Carl Zeiss light microscope (model Axiotop 40). For images on creased samples, the crease was made on the paperboard in the machine direction (MD) and cross direction (CD) in a Creaser perforator GPM 450. The creased samples were then folded to 180° and the cross-sectional images were taken. To reveal any fracture of the coated paperboard and creased samples, turpentine stained with Sudan red was brushed on the coated side and any signs of immediate penetration marks on the opposite side were determined.

2.8. Scanning Electron Microscopy. A Jeol JSM-IT500 variable pressure scanning electron microscope was used to investigate the surface morphology of the film. To obtain cryo-fractured cross sections, thin strips from the paperboard were first cut in the MD. Then, a small cut was made in the middle of the strip (along the thickness). The strip was subsequently dipped in liquid nitrogen and then bent and broken into two parts. These were glued to a disc sample holder with the fractured surface upward using carbon glue. The samples were coated with a thin gold layer and then viewed at a 5 kV acceleration voltage using the secondary electron detector.

2.9. Determination of WVTR. The gravimetric method was used to determine the water vapor transmission rate (WVTR). Open mouth test cups of 10 cm diameter were used with anhydrous calcium chloride as desiccant. Samples were mounted on these test cups, followed by sealing the cups with water proof wax. The cups, stored in a chamber (ESPEC, Model PR-2J) at 50% RH and 23 °C, were then weighed two times a day until steady-state WVTR was reached. WVTR was obtained as the mass increase of the cup, normalized to the sample exposure surface area and time. The WVTR values were normalized to the thickness to obtain the specific WVTR (sWVTR) which was expressed in g·mm/(m^2·day). Five replicates were used.

2.10. Determination of OP. The oxygen transmission rate (OTR) was determined using a MOCON Analyzer (Mocon OX-TRAN, model 2/21, MH module) at 50% RH and 23 °C. The samples were sandwiched between two aluminum foils with a circular exposure area of 5 cm^2. The samples were then brought in contact with 10% oxygen on the coated side of the paperboard and the amount of oxygen (in cm^3) that diffused through the sample was measured. The OTR was obtained by normalizing the oxygen penetrated to the sample surface exposure area and time and the OP was calculated by normalizing the values to film thickness and oxygen pressure difference over the film (1 atm). Two replicates were used.

2.11. Grease Resistance. The grease resistance of samples was measured using the ASTM-F119-82 method. Films were placed on fluorescent thin-layer chromatography (TLC) sheets marking test points. For each test point, two flannel pieces containing olive oil (six drops of olive oil pipetted on these) were placed on it with weights of 50 g and 2 mm diameter on top. The setup was then placed in an oven at 40 °C. The time taken for the oil to penetrate the sample was determined by detecting a darkening/color change on the TLC sheet at the test points (under ultraviolet light). Four test points were used for each film.

2.12. Determination of Adhesion Strength. Testometric M500 Texture Analyser was used to determine the peel strength of samples according to the T-peel test described in ASTM D1876. Rectangular strips with a width of 15 mm and a length of 200 mm were cut out in MD. Then, the extruded layer was separated from the coated paperboard manually, exposing a length of approximately 50 mm. The peeled polymer layer and the paperboard, referred to as peel arms, were clamped in the tensile tester, equipped with a 100 N load cell, and was pulled apart. The grip-to-grip distance ranged from 277 to 900 mm and the strain rate was 25 mm/min. The force was measured at each 20 mm, resulting in three values from one sample when pulled over a length of 70 mm. The peel strength was calculated as the average force required to pull the peel arms apart during the test per unit width of sample and was expressed as N/m. Two replicates were used.

2.13. Contact Angle Measurement. The contact angle of the highly polar water and medium polar ethylene glycol on the PFJ coated paperboards, with and without corona pretreatment, were measured using a KRUSS Drop Shape Analyzer—DSA100 at 23 °C and 50% relative humidity.

2.14. Heat bar Sealing. A KOPP Laboratory sealer SGPE 20 was used to study the heat bar sealing properties of the coated paperboard. The paperboard samples, with the coated side face-to-face were placed and sealed in between continuously heated, sealing, and supporting jaws for a duration of 1 s. After cooling to room temperature, the

https://doi.org/10.1021/acsapm.2c00153
ACS Appl. Polym. Mater. 2022, 4, 4179−4188

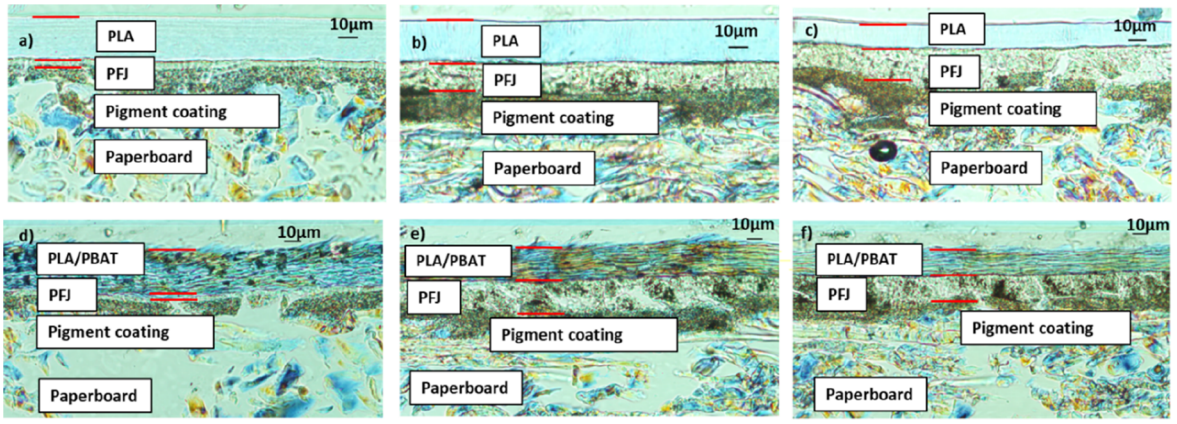

Figure 3. Cross-sectional images of paperboard with multilayer coating of (a) P0-thin-30PLA, (b) P0-thick-30PLA, (c) P0-thick-20 PLA, (d) P0-thin-30PLA/PBAT, (e) P0-thick-30PLA/PBAT, and (f) P0-thick-20PLA/PBAT.

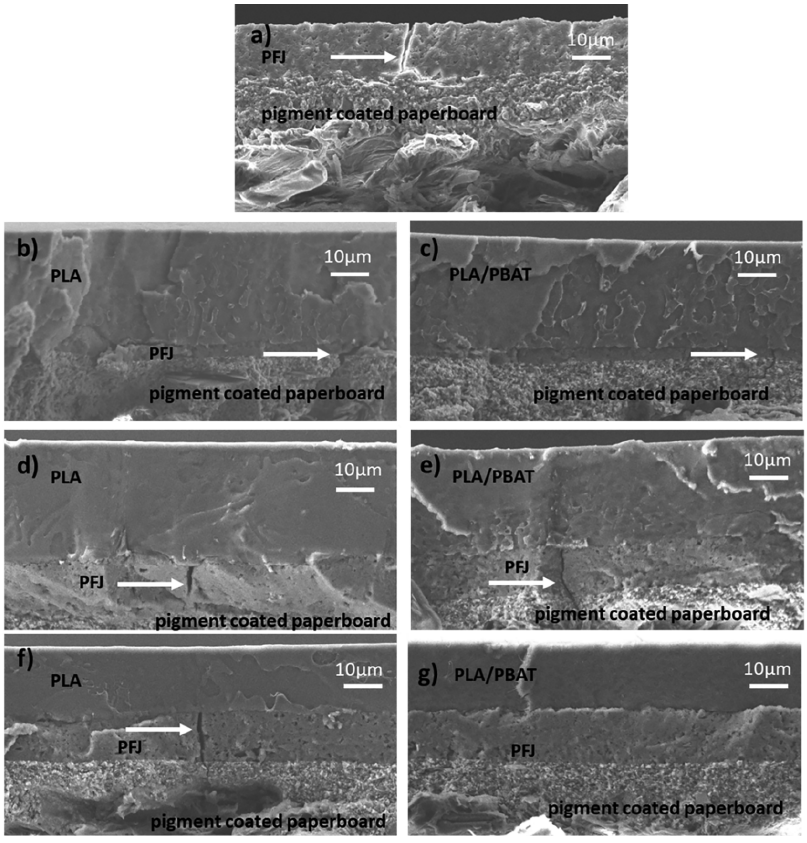

Figure 4. SEM images after cryofracture: (a) P0-thick, (b) P0-thin-30PLA, (c) P0-thin-30 PLA/PBAT, (d) P0-thick-30PLA, (e) P0-thick-30PLA/PBAT, (f) P0-thick-20PLA, and (g) P0-thick-20PLA/PBAT.

samples were teared apart to determine if any fiber-tear occurred. Different temperatures were tested and the minimum temperature that gave good cohesive failure (good fiber tear) was noted as the minimum heat-sealing temperature. All measurements were made in triplicates.

3. RESULTS AND DISCUSSION

3.1. Overall Coating Characteristics. Figure 2 shows the extrusion coated paperboard with PFJ as a middle layer between the paperboard and extrusion coating (with PLA or PLA/PBAT). The samples were homogeneous and glossy in appearance. The colorimeter values obtained are presented in Table 1.

A change in ΔE from ca. 28 for extrusion-coated thin PFJ-coated paperboards to 50 for extrusion-coated thick PFJ coated paperboards was observed. This was due to the decrease in the lightness (L^*) and the increase in the redness (a^*) and yellowness (b^*) with the PFJ coating thickness. This implies that as the PFJ coating became thicker, the paperboard became darker, as also observed in Figure 2.

The scanning electron microscopy (SEM) images of the surfaces are given in Figure S1. The images show some cracks and holes in the PFJ-coated paperboard. The existence of holes was confirmed by brushing turpentine stained with Sudan red on the coated side and noticing its immediate penetration to the other side of the paperboard. However, the PLA- or PLA/

https://doi.org/10.1021/acsapm.2c00153
ACS Appl. Polym. Mater. 2022, 4, 4179−4188

PBAT-coated paperboards had smoother surfaces with the absence of cracks and holes. This was also confirmed by the absence of immediate penetration marks on the other side of the paperboard, when tested with turpentine/Sudan red. Figure 3 shows the cross-sectional images for PLA- and PLA/PBAT-coated paperboards obtained with optical microscopy. The images show continuous and relatively uniform layers on the paperboard.

The PFJ layers were broken during creasing of the paperboard coated with only PFJ layers, whereas in the extrusion-coated PFJ samples, the PLA or PLA/PBAT layers were less affected. Figure S2 shows how the extrusion coating was stretched out in the crease region but did not fracture. The creased paperboards were tested for any damage by applying turpentine/Sudan red on the coated side. The PFJ-coated samples showed a clear immediate penetration mark along the crease, which was not the case for the extrusion-coated samples. The reason for the penetration marks can be explained based on the images in Figures S1 and 4. The PFJ layer contained occasional through-thickness cracks, which, without the extrusion-coated layer led to the ink penetration. Nevertheless, Figures 3 and 4 show that the different layers were uniform over the paperboard surface, as also shown by the low variation in the grammage and the layer thicknesses given in Tables S2 and S3.

The glass transition temperature of the extrusion-coated PLA and PLA in the PLA/PBAT blend was 62 °C and melting temperatures of PLA and PLA in the PLA/PBAT blend were 149 and 167 °C, respectively. The difference in melting point was due to that the PLA resins were not the same in the pure PLA and in the PLA/PBAT blend (Figure 5). The glass transition temperature of PBAT was below the measured ranged (reported to be—33.2 °C[21]). The degree of crystallinity of PLA was calculated using eq 2.

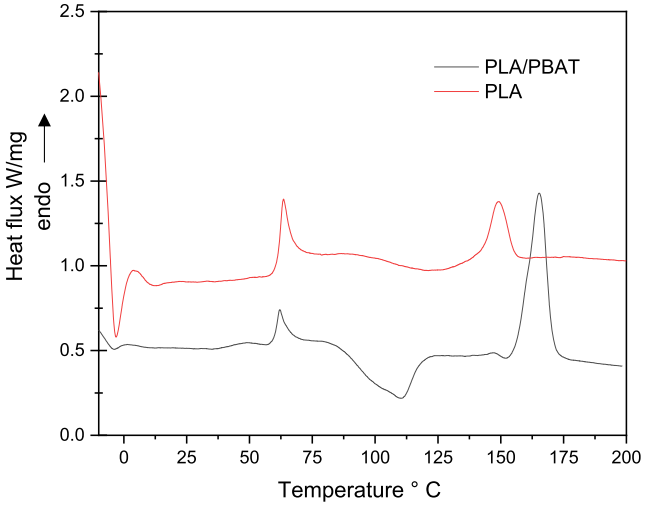

Figure 5. DSC curves of PLA and PLA/PBAT coating, obtained from the first heating scan.

$$X_c = (\Delta H_m - \Delta H_c)/(\phi \cdot \Delta H_c^*) \quad (2)$$

where X_c is the degree of crystallinity, ΔH_m is the melting enthalpy, and ΔH_c is the cold-crystallization enthalpy obtained from the DSC curves. ϕ is the weight fraction of PLA in the material and ΔH_c^* is the enthalpy of 100% crystalline PLA (80 J/g).[22] Equation 2 yielded a crystallinity of 1.3% for the PLA coating, hence an essentially amorphous material. The crystallinity of the blend (ϕ = 0.6) was more difficult to determine. Arruda et al.[21] reported a melting temperature between 60 and 126 °C for PBAT and no cold crystallization in blown films. In the present PLA/PBAT blends, a small shoulder at ca. 50 °C was discernible and possibly due to PBAT melting. However, it may also have appeared at a higher temperature, but not discernible in the DSC curve (Figure 5). Hence, in order to get a rough estimate about the overall crystallinity in the PLA/PBAT blend, eq 2 was used assuming that only the PLA was melting and cold-crystallizing. This yielded a crystallinity of 18%. Thus, despite the assumptions made, the crystallinity was higher in the PLA/PBAT blend, but still on a relatively low degree. It has been reported that PBAT can act as a nucleating agent for PLA, increasing its crystallization rate,[23] and that may also have been the case here, considering the earlier cold crystallization in the blend (Figure 5).

The presence of PBAT in blown films has been reported to yield significantly higher oxygen and water vapor permeabilities, compared to pure PLA, and it is clear that the main effect of adding PBAT to PLA is to increase the molecular mobility (consider their very different glass transitions, PBAT is rubbery and PLA glassy under ambient conditions).[23]

3.2. Water Vapor Transmission Rate. The WVTR and sWVTR of the paperboard, with and without coatings, are depicted in Table 2. Compared to the uncoated paperboard, having an sWVTR rate of 88 g·mm/(m^2·day), all coated samples showed significantly lower values. With the thin PFJ coating, the sWVTR was 25−28 g·mm/(m^2·day), which decreased further to 8 g·mm/(m^2·day) using a thick PFJ coating. However, the

Table 2. Water Vapor Barrier Properties[a]

reference and PFJ-coated paperboards	WVTR values (g/m^2·day)	sWVTR (g·mm/m^2·day)
reference-Ensocoat	266.5 ± 2.4	87.9 ± 0.8
P0-thin	80.6 ± 2.5	27.0 ± 0.8
P10-thin	75.8 ± 2.4	25.4 ± 0.8
P20-thin	84.9 ± 3.9	28.4 ± 1.3
P30-thin	79.7 ± 3.1	26.7 ± 1.0
P0-thick	22.7 ± 0.7	7.8 ± 0.2
P10-thick	24.0 ± 0.8	8.3 ± 0.3
P20-thick	24.4 ± 1.3	8.4 ± 0.4
P30-thick	23.9 ± 0.5	8.2 ± 0.2

	PLA coated		PLA/PBAT coated	
paperboards with extrusion coating	WVTR	sWVTR	WVTR	sWVTR
ref 30-*	43.4 ± 0.7	15.4 ± 0.3	54.2 ± 1.6	19.2 ± 0.6
P0-thin-30-*	20.3 ± 0.2	7.3 ± 0.1	24.8 ± 0.4	8.9 ± 0.1
P10-thin-30-*	19.3 ± 0.7	6.9 ± 0.3	22.7 ± 0.8	8.2 ± 0.3
P20-thin-30-*	19.0 ± 1.0	6.8 ± 0.4	21.1 ± 0.5	7.6 ± 0.2
P30-thin-30-*	18.1 ± 0.4	6.5 ± 0.2	21.3 ± 0.4	7.6 ± 0.1
P0-thick-30-*	11.4 ± 1.0	4.2 ± 0.4	12.0 ± 1.0	4.4 ± 0.4
P10-thick-30-*	10.8 ± 0.9	4.0 ± 0.3	10.7 ± 0.5	4.0 ± 0.2
P20-thick-30-*	10.9 ± 0.6	4.0 ± 0.2	10.0 ± 0.4	3.7 ± 0.1
P30-thick-30-*	10.4 ± 0.3	3.8 ± 0.1	11.0 ± 1.1	4.0 ± 0.4
ref 20-*	60.7 ± 2.0	21.0 ± 0.7	75.5 ± 1.1	26.7 ± 0.4
P0-thick-20-*	12.4 ± 0.1	4.5 ± 0.1	13.0 ± 0.8	4.7 ± 0.3
P10-thick-20-*	12.2 ± 0.3	4.4 ± 0.1	13.0 ± 1.3	4.7 ± 0.5
P20-thick-20-*	11.2 ± 0.1	4.0 ± 0.1	12.3 ± 0.3	4.4 ± 0.1
P30-thick-20-*	11.3 ± 0.4	4.1 ± 0.1	13.1 ± 1.2	4.7 ± 0.4

[a]-* refers to either PLA or PLA/PBAT coating.

https://doi.org/10.1021/acsapm.2c00153
ACS Appl. Polym. Mater. 2022, 4, 4179−4188

Table 3. Oxygen Barrier Properties[a]

	PLA coated		PLA/PBAT coated	
samples	OTR cm3/(m^2·day·atm)	OP cm^3·mm/(m^2·day·atm)	OTR cm3/(m^2·day·atm)	OP cm^3·mm/(m^2·day·atm)
ref 30*	1076 ± 10.8	381.2 ± 3.8	1577.9 ± 40.7	558.6 ± 14.4
P0-thin-30*	512.1 ± 103.5	183.8 ± 37.1	448.3 ± 57.6	160.9 ± 20.7
P10-thin-30*	542.2 ± 8.4	194.6 ± 3.0	320.1 ± 3.6	114.9 ± 1.3
P20-thin-30*	176.1 ± 7.4	63.2 ± 2.6	237.5 ± 29.6	85.3 ± 10.6
P30-thin-30*	125.0 ± 29.6	44.9 ± 10.6	198.9 ± 19.3	71.4 ± 6.9
P0-thick-30*	46.6 ± 17.9	17.2 ± 6.6	117.3 ± 23.8	43.4 ± 8.8
P10-thick-30*	32.6 ± 2.3	12.1 ± 0.9	42.7 ± 9.4	15.8 ± 3.5
P20-thick-30*	31.5 ± 0.6	11.6 ± 0.2	32.4 ± 0.1	12.0 ± 0.1
P30-thick-30	33.8 ± 0.7	12.5 ± 0.2	36.8 ± 2.4	13.6 ± 0.9
ref 20*	1242.5 ± 115.7	429.9 ±± 40.0	2770.1 ± 147.7	958.5 ± 51.5
P0-thick-20*	52.4 ± 0.6	19.0 ± 0.2	130.6 ± 76.4	47.3 ± 27.6
P10-thick-20*	32.7 ± 0.2	11.8 ± 0.1	80.6 ± 5.6	29.2 ± 2.0
P20-thick-20*	39.3 ± 1.5	14.2 ± 0.5	45.2 ± 7.9	16.4 ± 2.9
P30-thick-20*	31.9 ± 1.3	11.5 ± 0.5	29.8 ± 1.2	10.8 ± 0.4

[a]-* refers to either PLA or PLA/PBAT coating.

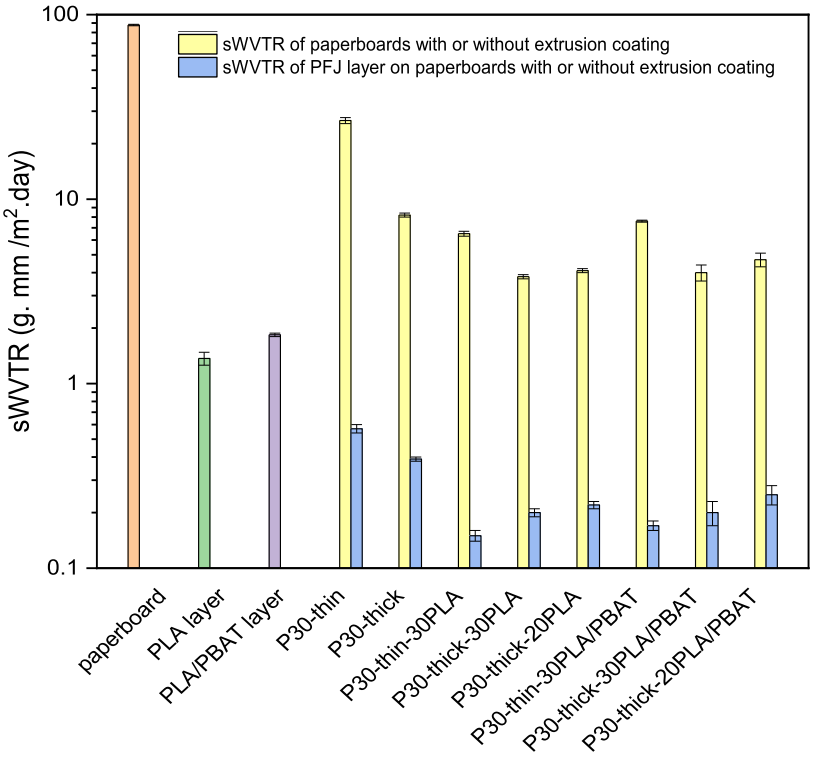

Figure 6. Effect of the PFJ layer on the sWVTR of the multilayer system.

glycerol content in the PFJ coating did not show any significant effect on the WVTR of the samples.

A decrease in WVP (water vapor permeability) is reported by Khwaldia et al.,[24] who coated paperboard [having a WVP of ca. 18 g.mm/(m^2·day·kPa)] with caseinate. As the coat weight (of 7% caseinate) increased from 5 to 16 g/m^2, the WVP decreased from approximately 13 to 6 g·mm/(m^2·day·kPa). Likewise, in the present PFJ-coated paperboards, a decrease in sWVTR from ca. 26 to 8 g·mm/m^2·day was noted when the grammage was increased from ca. 7 to 26 g/m^2 (a reduction of 70%).

With the combination of PFJ and an extrusion-coated layer, it was possible to reduce the sWVTR further, with the lowest values of ca. 4 g·mm/(m^2·day). When combining the thick PFJ coating with an extrusion-coated layer of 30 g/m^2 PLA or PLA/PBAT, the reduction was ~95% with respect to the paperboard value.

In a study using a cellulose-nanocrystal (CNC) (7 μm thick) and PLA (19 μm thick) two-layer coating on paper, by Koppolu et al.,[13] a WVTR of 28 g/(m^2·day) was reported at 23 °C and 50% RH. This is slightly higher than for the paperboard with only the thick PFJ layer here (Table 2). They also reported that low-density polyethylene (LDPE)-coated paperboard (of coating thickness 16 μm) had an sWVTR of 10 g/(m^2·day), which was similar to the values of samples here having a thick PFJ layer and 30 g/m^2 PLA or PLA/PBAT.

3.3. Oxygen Transmission Rate. The OP values are shown in Table 3. The uncoated paperboard and the PFJ-coated samples, without an extrusion coating, had OTR values too high

https://doi.org/10.1021/acsapm.2c00153
ACS Appl. Polym. Mater. 2022, 4, 4179−4188

to be measured. The high values for PFJ can be explained by the occasional cracks in this thin layer. However, when sandwiched between the extrusion-coated layer and the paperboard, the PFJ layer reduced significantly the OTR and OP values. Note especially the reduction in OP for the 20 g/m^2 PLA or PLA/PBAT extrusion-coated paperboard samples in the presence of the thick PFJ layer (Table 3). With the PFJ layer, the OP decreased from ca. 381 (PLA) and 558 (PLA/PBAT) to, at the best, ca. 11 cm^3·mm/(m^2 day·atm), representing a decrease by 97 and 98%, respectively. Considering the whole glycerol range (0−30%), the permeability decreased with the increase in glycerol content, reflecting the more uniform PFJ layer in the presence of glycerol. However, no difference in crack content was seen in the samples with varying glycerol content.

Kjellgren et al.[25] studied the OP of polyethylene extrusion-coated (coat weight 30 g/m^2) grease-proof paper with grammage 45 g/m^2 and reported OTR values of 230 and 1340 cm^3/(m^2 day atm) for sulfite and sulfate paper, respectively. These values are substantially higher than the OTR of our samples with a thick PFJ coating which was ca. 30 cm^3/(m^2 day atm) for both PLA and PLA/PBAT, independent of the extrusion-coating layer thickness.

3.4. Effect of PFJ Layer on sWVTR and OP Values in the Multilayer Systems. The effect of the PFJ layer on the total sWVTR and OP values of the coated paperboard was determined using the laminate equation (eq 3).[26]

$$Q_{\text{total}} = \frac{l_{\text{total}}}{\left(\frac{l_{\text{paperboard}}}{Q_{\text{paperboard}}} + \frac{l_{\text{PFJ}}}{Q_{\text{PFJ}}} + \frac{l_{\text{PLA or PLA/PBAT}}}{Q_{\text{PLA or PLA/PBAT}}}\right)} \quad (3)$$

where Q is the sWVTR or OP and l is the thickness of each layer. Q_{total} represents the total sWVTR or OP of the coated paperboard and l_{total} is the total thickness. The calculated sWVTR and OP for the PFJ layer (Q_{PFJ}) is compared with the total permeability values of the multilayer-coated paperboard (with 30% glycerol content in PFJ) in Figures 6 and 7. The values of all samples are listed in Tables S4 and S5.

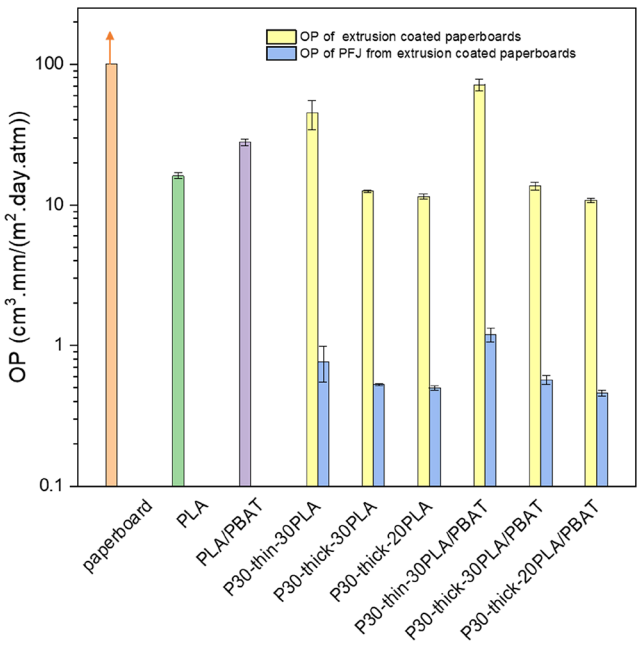

Figure 7. Effect of the PFJ layer on the OP of the multilayer system.

The sWVTR values of the PFJ layer in these laminates were better (down to 0.15 g·mm/m^2·day) than in the PFJ films developed in the work reported, which was in the range of 5−13 g·mm/m^2·day.[18] This was most likely due to that the layer here was protected by the PLA or PLA/PBAT layer, and the PFJ water uptake was therefore less in the laminate layer than that in the pure films. However, also the PFJ layer without the extrusion-coating was lower (less than 1 g·mm/m^2·day) than for the free-standing films in the previous work, which can be due to that the coating could not swell freely on the paperboard.

sWVTR of PFJ in PFJ-coated paperboard [0.3 to 0.5 g·mm/(m^2·day)] was similar to the sWVTR of wheat gluten in gluten-coated paperboards [ca. 0.5 g·mm/(m^2·day)], as reported by Türe et al.[27]

In the previous work, the OP values of the PFJ films were as low as 0.01 cm^3·mm/(m^2·day·atm).[18] In contrast to that in the paper coatings with only PFJ, the OP values were too high to be measured due to cracks and pinholes present in the thin coatings (as shown in Figure S1). This is also most likely the reason for the higher OP values of the individual PFJ layers in the extrusion-coated paperboards. Even though the coated samples had small cracks and holes, it was showing less sWVTR, but high OP. This is due to the fact that water transport is not as sensitive to occasional cracks or holes because of its high surface energy/tension and OP is very sensitive to these small cracks and holes. Another reason for differences between the transport properties in the previous and the present work can be differences in the properties of PFJ in different batches. It is always a risk that the properties of natural materials can vary from batch to batch.

The PFJ layer exhibited OP values of ca. 0.5 to 14 cm^3·mm/(m^2·day·atm), which was comparable to those of the OP values for the wheat gluten layer in wheat gluten/PLA laminates [between ca. 0.007 and 6.9 cm^3·mm/(m^2·day·atm)] as reported by Cho et al.[28]

3.5. Grease Resistance Test. The paperboard showed a grease penetration on TLC sheets already after 2 h from the start of the test. When coated with a thin and thick PFJ layer the penetration occurred after 5 h. Considerably longer penetration times (12 days) was observed for the paperboard having either the PLA or the PLA/PBAT extrusion-coated layer. Paperboards with a thin coating of PFJ and 30 g/m^2 extrusion-coating showed penetration marks after 14 days. With a thick PFJ layer between the paperboard and the extrusion-coated layer the penetration did not occur until after a month (31 days).

Koppolu et al.[13] reported that it took 6 days for an LDPE-coated (with a thickness of 16 μm and a grammage of 14 g/m^2) paperboard (grammage of 204 g/m^2) to experience the first penetration mark using the same method as here. It is promising that the samples here had better grease barrier properties than the LDPE-coated paperboard.

3.6. Peel Strength. The peel strength of the extrusion-coated paperboards is presented in Table 4. The 30 and 20 g/m^2 PLA-coated paperboards without PFJ showed adhesion strengths of 21 and 17 N/m, respectively. The PLA/PBAT-coated paperboard exhibited peel strengths of 37 and 32 N/m for, respectively, the 30 and 20 g/m^2 PLA/PBAT coatings. Hence, the PLA/PBAT coating showed, in general, better adhesion to the paperboard compared to the PLA layer, with or without the PFJ layer in between. The PLA/PBAT being softer compared to PLA may form an overall tighter connection to the paperboard. Differences in chemical attraction between the polymers and paperboard could also affect the adhesion.

https://doi.org/10.1021/acsapm.2c00153
ACS Appl. Polym. Mater. 2022, 4, 4179−4188

Table 4. Peel Strength of Coated Paperboards[a]

	peel strength (N/m)	
extrusion-coated paperboards	PLA coated	PLA/PBAT coated
ref 30*	21.0 ± 1.5	37.3 ± 1.1
P0-thin-30*	5.4 ± 4.4	17.3 ± 1.8
P10-thin-30*	8.4 ± 0.5	23.1 ± 1.3
P20-thin-30*	8.8 ± 2.3	22.6 ± 2.1
P30-thin-30*	9.2 ± 4.6	21.4 ± 2.3
P0-thick-30*	20.6 ± 1.4	31.5 ± 3.0
P10-thick-30*	16.6 ± 0.3	27.6 ± 1.3
P20-thick-30*	15.1 ± 7.5	21.3 ± 1.6
P30-thick-30*	16.6 ± 1.1	18.1 ± 9.0
P0-thick-30*-without corona	8.0 ± 1.5	12.3 ± 1.4
P10-thick-30*-without corona	6.5 ± 1.1	9.8 ± 4.8
P20-thick-30*-without corona	9.1 ± 1.7	13.3 ± 1.6
P30-thick-30*-without corona	10.2 ± 1.6	11.5 ± 5.7
ref 20*	17.2 ± 13.4	31.6 ± 3.0
P0-thick-20*	21.3 ± 0.6	19.4 ± 1.2
P10-thick-20*	21.1 ± 1.8	19.3 ± 1.5
P20-thick-20*	14.4 ± 11.2	15.4 ± 7.5
P30-thick-20*	19.4 ± 0.6	19.1 ± 9.5

[a]-* refers to either PLA or PLA/PBAT coating.

Moreover, it was noted from the results that the peel strength became, in general, weaker when a PFJ layer was placed between the extrusion-coated layer and the paperboard, compared to without the PFJ layer. The PFJ layer prevented the extruded layer to wet and fill the pores in the paperboard resulting in weaker peel strength. However, also in general, the thicker PFJ layer yielded higher peel strength than that of the thinner PFJ layer. A possible reason to this is that the thicker PFJ layer had a smoother surface than the thin one, thereby leading to a larger contact area to the adjacent layers and higher peel strength.

It was also noted that the extrusion-coated layer, when separated from the coated paperboard, exhibited no fiber tear (Figure S3). The FTIR curves shown in Figure S4 showed that the PFJ remained on the paperboard after peeling the extrusion-coated layer, when no corona was used. However, the peeled PLA and PLA/PBAT layers from the corona-treated PFJ/paperboard showed traces of PFJ on the side toward the paperboard. Hence, the experiments on the paperboards with a thick PFJ and 30 g/m^2 extrusion-coated layer showed that the corona pre-treatment was important and improved the peel strength. It increased the oxidation/polarity of the PFJ-coated paperboard, resulting in better adhesion between the PFJ/paperboard and the extrusion coating. It was not possible to assess directly the increase in surface energy after the corona treatment because the water and ethylene glycol droplets were absorbed with time by the PFJ layer. However, the decrease in the contact angle with the corona treatment, as observed after a short time (1 s), indicated an increasing surface energy/polarity of the PFJ-coated paperboard (Figure S5).

A similar trend of an increase in adhesion of paperboard and LDPE (with a grammage of 20 g/m^2) when pretreated with corona was reported by Kuusipalo and Savolainen.[29] They also reported an increase in peel strength from 3 to 23 and 9 to 38 N/m, when adding a corona pretreatment to a folding boxboard (grammage: 205 g/m^2) extrusion-coated with a polypropylene homo- and co-polymer, respectively.

3.7. Heat Sealing Test. Bar sealing test was done for the paperboards coated with PLA or PLA/PBAT. For PLA-coated samples with only a 30 g/m^2 PLA-coating on the paperboard, the minimum heat-sealing temperature was 80 °C. A thin PFJ-coating beneath the same extrusion-coated layer increased the minimum heat-sealing temperature to 140 °C. The use of a thick PFJ coating combined with the same PLA coating failed to yield good fiber tear at any temperature. For the samples with only a PLA/PBAT extrusion-coating on paperboard, the minimum heat-sealing temperature attained was 90 °C. In the presence of either a thin or a thick PFJ coating together with the extruded PLA/PBAT-layer, the minimum heat-sealing temperature increased to 120 °C. At lower temperature adhesion failure occurred between the PFJ and PLA layer, which was confirmed by the absence of good fiber tear when the sealed paperboards were teared apart. When the temperature was increased the adhesion between the PLA or PLA/PBAT and PFJ layer also increased, which was observed by good fiber tear. To conclude, overall, the PLA/PBAT/PFJ-coated paperboards were easier to heat seal compared to those with a PLA extrusion-coated layer.

4. CONCLUSIONS

This is the first study to explore the possibility of PFJ as a barrier coating material on the paperboard, with and without an extrusion-layer of PLA or PLA/PBAT on top. The paperboard was rod-coated with PFJ, followed by extrusion-coating a layer of PLA or PLA/PBAT on top. This latter step served to protect the hydrophilic PFJ layer from moisture. The water vapor transport was significantly reduced with a PFJ layer present and further reduced with the presence of an extrusion-coated layer. The OP was reduced significantly when a PFJ layer was placed between the extrusion-coated layer and the paperboard. In brief, the coated paperboards showed very promising both water vapor and oxygen barrier properties. Among the different combinations investigated, the paperboards with a thick PFJ layer and a 30 g/m^2 PLA or PLA/PBAT layer yielded the best barrier properties. The corona treatment helped to achieve better adhesion of the coating to the paperboard, with PLA/PBAT exhibiting better adhesion compared to PLA on PFJ-coated paperboards. The PFJ with the PLA/PBAT-coated paperboards were showing good heat-sealing properties as well. The results presented indicated that the developed bio-based multilayer coatings show competitive properties to petroleum-based polymer coatings and they are promising as a solution for barrier coatings on paperboard.

■ ASSOCIATED CONTENT

Supporting Information

The Supporting Information is available free of charge at https://pubs.acs.org/doi/10.1021/acsapm.2c00153.

Identification of samples; grammage of coated and uncoated paperboards; thickness of the paperboard and the coated layers; effect of the PFJ layer on sWVTR of the multilayer system; effect of PFJ layer on OP on the multilayer system; SEM images showing surfaces of the paperboard; optical microscopy images after creasing; peeled extrusion-coated layer from the paperboard with corona treatment; FTIR curves of the extrusion layer and paperboard after peeling off the PLA and PLA/PBAT; and contact angles of water and ethylene glycol before and after corona treatment of the PFJ-coated paperboard (PDF)

https://doi.org/10.1021/acsapm.2c00153
ACS Appl. Polym. Mater. 2022, 4, 4179−4188

AUTHOR INFORMATION

Corresponding Authors

Simi Poulose − *Faculty of Engineering and Natural Sciences, Materials Science and Environmental Engineering, Tampere University, FI-33014 Tampere, Finland;* orcid.org/0000-0003-1407-3756; Email: simi.poulose@tuni.fi

Mikael S. Hedenqvist − *Department of Fibre and Polymer Technology, School of Engineering Sciences in Chemistry, Biotechnology and Health, KTH Royal Institute of Technology, SE-100 44 Stockholm, Sweden;* orcid.org/0000-0002-6071-6241; Email: mikaelhe@kth.se

Authors

Juuso Toriseva − *Faculty of Engineering and Natural Sciences, Materials Science and Environmental Engineering, Tampere University, FI-33014 Tampere, Finland*

Johanna Lahti − *Faculty of Engineering and Natural Sciences, Materials Science and Environmental Engineering, Tampere University, FI-33014 Tampere, Finland*

Ilari Jönkkäri − *Faculty of Engineering and Natural Sciences, Materials Science and Environmental Engineering, Tampere University, FI-33014 Tampere, Finland*

Jurkka Kuusipalo − *Faculty of Engineering and Natural Sciences, Materials Science and Environmental Engineering, Tampere University, FI-33014 Tampere, Finland*

Complete contact information is available at: https://pubs.acs.org/10.1021/acsapm.2c00153

Author Contributions

The manuscript was written through contributions of all authors. All authors have given approval to the final version of the manuscript.

Notes

The authors declare no competing financial interest.

ACKNOWLEDGMENTS

We convey our gratitude to Finnamyl Oy., Finland and Stora Enso for kindly providing us with PFJ and pigment-coated paperboard, respectively. Financial support from The Faculty of Engineering and Natural Sciences, Tampere University is gratefully acknowledged. This work made use of Tampere Microscopy Center facilities at Tampere University and authors would like to thank their support.

ABBREVIATIONS

PFJ, potato fruit juice; PLA, poly(lactic acid); PBAT, poly(butylene adipate terephthalate); EVOH, poly(ethylene-*co*-vinyl alcohol); PVDC, polyvinylidene chloride; PHB, poly(hydroxy butyrate); wt %, weight percentage; RH, relative humidity; MD, machine direction; CD, cross direction; DSC, differential scanning calorimetry; SEM, scanning electron microscopy; WVTR, water vapor transmission rate; sWVTR, specific water vapor transmission rate; WVP, water vapor permeability; OP, oxygen permeability; OTR, oxygen transmission rate; CNC, cellulose-nanocrystal; LDPE, low-density polyethylene; TLC, thin-layer chromatography

REFERENCES

(1) Gällstedt, B. M.; Brottman, A.; Hedenqvist, M. S. Packaging-Related Properties of Protein- and Chitosan-Coated Paper and Science. *Packag. Technol. Sci.* **2005**, *18*, 161−170.

(2) Andersson, C. New Ways to Enhance the Functionality of Paperboard by Surface Treatment - A Review. *Packag. Technol. Sci.* **2008**, *21*, 339−373.

(3) Rastogi, V.; Samyn, P. Bio-Based Coatings for Paper Applications. *Coatings* **2015**, *5*, 887−930.

(4) Han, J. H.; Krochta, J. M. Physical Properties and Oil Absorption of Whey-Protein-Coated Paper. *J. Food Sci.* **2001**, *66*, 294−299.

(5) Park, H. J.; Kim, S. H.; Lim, S. T.; Shin, D. H.; Choi, S. Y.; Hwang, K. T. Grease Resistance and Mechanical Properties of Isolated Soy Protein-Coated Paper. *J. Am. Oil Chem. Soc.* **2000**, *77*, 269−273.

(6) Cho, S.-W.; Blomfeldt, T. O. J.; Halonen, H.; Gällstedt, M.; Hedenqvist, M. S. Wheat Gluten-Laminated Paperboard with Improved Moisture Barrier Properties: A New Concept Using a Plasticizer (Glycerol) Containing a Hydrophobic Component (Oleic Acid). *Int. J. Polym. Sci.* **2012**, *2012*, 454359.

(7) Guillaume, C.; Pinte, J.; Gontard, N.; Gastaldi, E. Wheat Gluten-Coated Papers for Bio-Based Food Packaging: Structure, Surface and Transfer Properties. *Food Res. Int.* **2010**, *43*, 1395−1401.

(8) Nechita, P.; Roman, M. Review on Polysaccharides Used in Coatings for Food. *Coatings* **2020**, *10*, 566.

(9) Sothornvit, R. Effect of Hydroxypropyl Methylcellulose and Lipid on Mechanical Properties and Water Vapor Permeability of Coated Paper. *Food Res. Int.* **2009**, *42*, 307−311.

(10) N, S.; S, A. K.; A, P.; S, G. Studies on Semi-Crystalline Poly Lactic Acid (PLA) as a Hydrophobic Coating Material on Kraft Paper for Imparting Barrier Properties in Coated Abrasive Applications. *Prog. Org. Coat.* **2020**, *145*, 105682.

(11) Erkske, D.; Viskere, I.; Dzene, A.; Tupureina, V.; Savenkova, L. Biobased Polymer Composites for Films and Coatings. *Proc. Est. Acad. Sci.* **2006**, *55*, 70−77.

(12) Song, Z.; Xiao, H.; Zhao, Y. Hydrophobic-Modified Nano-Cellulose Fiber/PLA Biodegradable Composites for Lowering Water Vapor Transmission Rate (WVTR) of Paper. *Carbohydr. Polym.* **2014**, *111*, 442−448.

(13) Koppolu, R.; Lahti, J.; Abitbol, T.; Swerin, A.; Kuusipalo, J.; Toivakka, M. Continuous Processing of Nanocellulose and Polylactic Acid into Multilayer Barrier Coatings. *ACS Appl. Mater. Interfaces* **2019**, *11*, 11920−11927.

(14) Wang, N.; Zhang, C.; Weng, Y. Enhancing Gas Barrier Performance of Polylactic Acid/Lignin Composite Films through Cooperative Effect of Compatibilization and Nucleation. *J. Appl. Polym. Sci.* **2021**, *138*, 50199.

(15) Li, F.; Zhang, C.; Weng, Y. Improvement of the Gas Barrier Properties of PLA/OMMT Films by Regulating the Interlayer Spacing of OMMT and the Crystallinity of PLA. *ACS Omega* **2020**, *5*, 18675−18684.

(16) Li, F.; Zhang, C.; Weng, Y.; Diao, X.; Zhou, Y.; Song, X. Enhancement of Gas Barrier Properties of Graphene Oxide/Poly (Lactic Acid) Films Using a Solvent-Free Method. *Materials* **2020**, *13*, 3024.

(17) van Koningsveld, G. A. Physico-Chemical and Functional Properties of Potato Proteins. PhD Thesis, Wageningen University, 2001.

(18) Poulose, S.; Jönkkäri, I.; Hedenqvist, M. S.; Kuusipalo, J. Bioplastic Films with Unusually Good Oxygen Barrier Properties Based on Potato Fruit-Juice. *RSC Adv.* **2021**, *11*, 12543−12548.

(19) Zhao, P.; Liu, W.; Wu, Q.; Ren, J. Preparation, Mechanical, and Thermal Properties of Biodegradable Polyesters/Poly (Lactic Acid) Blends. *J. Nanomater.* **2010**, *2010*, 287082.

(20) Scrinzi, E.; Rossi, S.; Deflorian, F.; Zanella, C. Evaluation of Aesthetic Durability of Waterborne Polyurethane Coatings Applied on Wood for Interior Applications. *Prog. Org. Coat.* **2011**, *72*, 81−87.

(21) Arruda, L. C.; Magaton, M.; Bretas, R. E. S.; Ueki, M. M. Influence of Chain Extender on Mechanical, Thermal and Morphological Properties of Blown Films of PLA/PBAT Blends. *Polym. Test.* **2015**, *43*, 27−37.

(22) Tsai, W.-C.; Hedenqvist, M. S.; Laiback, Å.; Melin, H.; Ngo, M.; Trollsås, M.; Gedde, U. W. Physical Changes and Sorption/Desorption

Behaviour of Amorphous and Semi-Crystalline PLLA Exposed to Water, Methanol and Ethanol. *Eur. Polym. J.* **2016**, *76*, 278−293.
(23) Pietrosanto, A.; Scarfato, P.; Di Maio, L.; Nobile, M. R.; Incarnato, L. Evaluation of the Suitability of Poly(Lactide)/Poly-(Butylene-Adipate-Co-Terephthalate) Blown Films for Chilled and Frozen Food Packaging Applications. *Polymers* **2020**, *12*, 804.
(24) Khwaldia, K.; Basta, A. H.; Aloui, H.; El-Saied, H. Chitosan-Caseinate Bilayer Coatings for Paper Packaging Materials. *Carbohydr. Polym.* **20142014**, *99*, 508−516.
(25) Kjellgren, H.; Stolpe, L.; Engström, G. Oxygen Permeability of Polyethylene-Extrusion-Coated Greaseproof Paper. *Nord. Pulp Pap. Res. J.* **2008**, *23*, 272−276.
(26) Lundbäck, M.; Hedenqvist, M. S.; Jansson, A.; Wirsén, A.; Albertsson, A.-C.; Gedde, U. W.; Hägglund, C.; Petersén, K. Hydrophobicity and Water Vapor Permeability of Ethylene-Plasma-Coated Whey, Chitosan and Starch Films. *Int. J. Polym. Mater. Polym. Biomater.* **2001**, *49*, 131−145.
(27) Türe, H.; Gällstedt, M.; Johansson, E.; Hedenqvist, M. S. Wheat-Gluten/Montmorillonite Clay Multilayer-Coated Paperboards with High Barrier Properties. *Ind. Crops Prod.* **2013**, *51*, 1−6.
(28) Cho, S.-W.; Gällstedt, M.; Hedenqvist, M. S. Properties of Wheat Gluten/Poly(Lactic Acid) Laminates. *J. Agric. Food Chem.* **2010**, *58*, 7344−7350.
(29) Kuusipalo, J.; Savolainen, A. Adhesion Phenomena in (Co)-Extrusion Coating of Paper and Paperboard. *J. Adhes. Sci. Technol.* **1997**, *11*, 1119−1135.

https://doi.org/10.1021/acsapm.2c00153
ACS Appl. Polym. Mater. 2022, 4, 4179−4188